



Synthesis of ordered mesoporous carbon materials and their catalytic performance in dehydrogenation of propane to propylene

Lei Liu^a, Qing-Fang Deng^a, Bao Agula^{a,b}, Tie-Zhen Ren^c, Yu-Ping Liu^d,
Bao Zhaorigetu^b, Zhong-Yong Yuan^{a,*}

^a Institute of New Catalytic Materials Science, Key Laboratory of Advanced Energy Materials Chemistry (Ministry of Education), College of Chemistry, Nankai University, Tianjin 300071, China

^b College of Chemistry and Environmental Science, Inner Mongolia Normal University, Huhhot 010022, China

^c School of Chemical Engineering and Technology, Hebei University of Technology, Tianjin 300130, China

^d Research Center for Analytical Sciences, College of Chemistry, Nankai University, Tianjin 300071, China

ARTICLE INFO

Article history:

Received 31 May 2011

Received in revised form 3 August 2011

Accepted 11 August 2011

Available online 3 September 2011

Keywords:

Ordered mesoporous carbon

Citric acid

Dehydrogenation

Propane

Propylene

ABSTRACT

Monolithic mesoporous carbons were prepared through a simple autoclaving method using citric acid as catalyst instead of HCl. The presence of citric acid plays an important role in determining the structural ordering of the resultant mesoporous structure due to the –COOH groups which can enhance hydrogen interaction between structural directing agent of triblock copolymer F127 and polymeric carbon precursor of resorcinol–formaldehyde resins. The obtained carbons have a hexagonal pore system, uniform pore size of ~5.0 nm and high BET surface area of ~758 m²/g. The prepared mesoporous carbons were used as catalyst for dehydrogenation of propane, exhibiting high catalytic activity and stability. After 50 h time-on-stream, the propane conversion of 12.1% was observed with propylene selectivity of 95.1% in the direct dehydrogenation process, while the propane conversion of 20.1% with propylene selectivity of 25.8% in oxidative dehydrogenation process. It has been found that the surface basic groups are active sites.

© 2011 Elsevier B.V. All rights reserved.

1. Introduction

Porous carbon materials have attracted much interest in catalysis, especially metal-free catalysis, due to their unique porous structure and chemical properties. During the last three decades, activated carbon (AC) itself was shown to be a promising catalyst for the oxidative dehydrogenation (ODH) reaction [1,2]. However, the commercialized AC as catalyst for ODH reaction is not possible, because its low stability in an oxidative atmosphere hindered the potential use of AC. Most recently, nanocarbons have been found to be efficient in ODH of ethylbenzene and alkanes [3–10], which provided a new way in the area of catalysis. With the large surface area and uniform pore sizes, mesoporous carbon materials offer possibility of creating reaction sites and molecular confinement that permit the selective formation of reaction products in heterogeneous catalysis. However, little effort to date has been focused on the dehydrogenation of propane to propylene over mesoporous carbon materials, although propylene is an indispensable raw material for numerous products.

Synthesis of ordered mesoporous carbon materials (OMCs) with various structures has achieved great progress. Nanocasting method from mesoporous silica is complicated, though it has been extensively developed to synthesize OMCs [11–13]. More recently, facile routes were developed to fabricate OMCs by assembly of block copolymers with polymeric carbon precursor followed by removal of block copolymers and carbonization [14–18]. Based on the organic–organic self-assembly, the OMCs obtained by the evaporation induced self-assembly method are always in the form of films [14–16]. Although such a synthesis of OMCs is a great improvement compared to nanocasting pathway, the direct preparation of mesoporous carbons with well-ordered pore system and perfect macroscopic morphology is still a great challenge. In our previous work, mesoporous carbons were obtained by using triblock copolymer F127 as template and resorcinol/formaldehyde resol as carbon precursor in the presence of HCl [19]. Herein, we report a facile one-pot approach in the aqueous phase under mild reaction conditions to synthesize mesoporous carbons with ordered mesoporous structure and perfect macroscopic morphology. The crucial difference to previous work is the presence of citric acid as catalyst which catalyzed both the formation of resorcinol–formaldehyde resol and the assembly of ordered mesostructure. The obtained ordered carbon samples were used as catalyst in the direct dehydrogenation (DH) and oxidative

* Corresponding author. Tel.: +86 22 23509610; fax: +86 22 23509610.
E-mail address: zyuan@nankai.edu.cn (Z.-Y. Yuan).

dehydrogenation (ODH) of propane to propylene. And it has been revealed that the mesoporous carbon catalyst can efficiently catalyze the dehydrogenation reaction, despite of no metal deposited, exhibiting high catalytic activity and stability.

2. Experimental

2.1. Synthesis

The OMCs were prepared through an autoclaving method with the molar ratio of formaldehyde to resorcinol of 2:1. In a typical synthesis, 1.65 g of resorcinol and 1.5 g of poly (ethylene oxide)-poly (propylene oxide)-poly (ethylene oxide) copolymer of Pluronic F127 (PEO₁₀₆-PPO₇₀-PEO₁₀₆, $M_w = 11,500$) was dissolved in a mixture of 20 mL of water and 20 mL of ethanol. 0.2 g of HCl (37%) or 2.1 g of citric acid was then added to the above solution. After 1 h of stirring, 2.5 g of 37% formaldehyde solution was added dropwise under tempustuously stirring, resulting in pH = 6.0–7.0 of the reaction system. The reaction mixture was then transferred to a Teflon-lined autoclave and heated at 60 °C for 2 days. The obtained products were collected by filtration, washed with water and dried, and then carbonized at 600 °C for 3 h. The final products were named as HOMC and COMC when HCl and citric acid were used as catalysts, respectively.

2.2. Characterization

Transmission electron microscopy (TEM) measurements were performed on a Philips Tecnai F20 microscope at 200 kV. All samples subjected to TEM measurements were ultrasonically dispersed in ethanol and drop-cast onto copper grids covered with carbon film. Small angle X-ray scattering (SAXS) experiments were performed on a Bruker Nanostar small angle X-ray scattering system. Nitrogen adsorption and desorption isotherms were measured on a Quantachrome NOVA 2000e sorption analyzer at 77 K. Before measurements, the samples were degassed in a vacuum at 200 °C for at least 6 h. The Brunauer–Emmett–Teller (BET) method was utilized to calculate the specific surface areas (S_{BET}), the pore size distributions were obtained using non-local density functional theory (NLDFT) method, and the total pore volumes (V_{total}) were estimated from the adsorbed amount at a relative pressure P/P_0 of 0.980. X-ray photoelectron spectroscopy (XPS) measurements were performed on a Kratos Axis Ultra DLD (delay line detector) spectrometer equipped with a monochromatic Al K_{α} X-ray source (1486.6 eV). All XPS spectra were recorded using an aperture slot of 300 $\mu\text{m} \times 700 \mu\text{m}$, survey spectra were recorded with a pass energy of 160 eV, and high-resolution spectra with a pass energy of 40 eV. The binding energies (BE) were referenced to the C 1s peak of contaminant carbon at 284.6 eV with an uncertainty of ± 0.2 eV. A Shirley background was subtracted before fitting. The full width at half maximum (FWHM) of the C1 peak was 1.0–1.2 eV, 2.0 ± 0.2 eV for the C2–C4 peaks and 2.5 ± 0.2 eV for the C5 peaks. The C1 peak had an asymmetrical shape, whereas the other peaks were symmetrical. The FWHM of the O 1s peak was 2.0 ± 0.3 eV for O1–O4. The Gauss–Lorentz ratio was maintained at values higher than 0.5. The temperature-programmed desorption (TPD) profiles were obtained from a Quantachrome CHEMBET-3000 analyzer, consisting of a U-shaped tubular micro-reactor, placed inside an electrical furnace. The mass flow rate of the helium carrier gas (20 mL/min) and the heating rate of the furnace (5 K/min) were controlled with appropriate units.

2.3. Catalytic testing

Catalytic tests were performed in a stainless steel, fixed-bed flow microreactor at atmospheric pressure. In the DH process,

the gas reactant contained 5 vol% propane and a balance of nitrogen (total flow rate = 40 mL/min). The operating temperature is between 673 and 873 K. ODH was performed with the gas reactant contained 10 vol% propane, 10 vol% oxygen and balancing nitrogen (total flow rate = 50 mL/min) at temperatures between 523 and 673 K with catalyst loading of 500 mg. Propane (C_3H_8) conversion and selectivity to products have been calculated as follows:

$$\text{C}_3\text{H}_8 \text{ Conversion (mol \%)} = \frac{\text{moles of C}_3 \text{ reacted}}{\text{moles of C}_3 \text{ fed}} \times 100$$

$$\text{Selectivity (mol \%)} = \frac{\text{moles of product i formed}}{\text{moles of C}_3 \text{ reacted}} \times \left(\frac{N_i}{N_{\text{C}_3}} \right) \times 100$$

3. Results and discussion

Organic–organic self-assembly depends on the hydrogen bonding between resins containing abundant hydroxyl groups and the polyethylene oxide (PEO) segments of the self-assembled triblock copolymers [14–19]. The previous reported works usually employed HCl as catalyst to polymerize the formation of phenol resin. However, much halogenide ions were introduced to the reaction system, which is not friendly to the environmental. In this work, citric acid was used to friendly catalyze the formation of resorcinol–formaldehyde resin and enhances the interaction between resins and F127, attributing to the abundant –COOH groups.

Photographs of the obtained monolithic polymer and the corresponding carbon materials are shown in Fig. 1. Short column-like polymer (Fig. 1a, diameter of approx. 21 mm and height of approx. 5 mm) can be obtained in the presence of citric acid. The shape and size of the obtained product can be easily tuned by changing the size of the Teflon-lined autoclave. Carbonization causes the color change of the polymer to black, but the shape is well retained, and the obtained short column-like carbon is crack-free, even an obvious shrinkage (31%) in size occurs (Fig. 1b, diameter of approx. 17 mm and height of approx. 3.5 mm).

In our previous work, it has been found that only poorly ordered mesostructure can be obtained when the molar ratio of formaldehyde to resorcinol fixed at 2:1 and autoclaving for 2 days if HCl was used as catalyst [19]. As the SAXS patterns shown in Fig. 1c, HOMC represents a wide and poorly resolved peak, suggesting a continuous structural distortion, though the orderly arranged pore structures can be observed in the TEM image (Fig. 1d). COMC shows a much stronger diffraction peak at q -value of 0.68 nm^{-1} that can be indexed as (10) reflection associated with 2D hexagonal $p6mm$ symmetry. The well ordered regularity is also observed in TEM image (Fig. 1e). This observation indicates that COMC has a higher degree of hexagonal mesoscopic organization than HOMC. Since the pH values of citric acid and HCl catalyzed reaction system are quite similar (pH = 6.0–7.0), it is clear that citric acid plays an important role in the formation of periodic mesostructure, attributing to the abundant –COOH groups in citric acid which may enhance the interaction between resorcinol and F127 [20]. The intense (10) peak of COMC reflects a d -spacing of 9.7 nm, which corresponds to a large unit-cell parameter ($a_0 = 11.2 \text{ nm}$).

The textural properties of mesoporous carbons were determined by the nitrogen sorption analysis. As exhibited in Fig. 2, the isotherms of the carbonized samples are of type IV with a clear hysteresis loop at $P/P_0 = 0.4$ – 0.7 , indicating mesoporous character. Meanwhile, the large volume adsorbed at the lower $P/P_0 = 0$ – 0.1 implies the presence of microporosity. Type-H1 hysteresis loops and narrow pore size distributions centered at around 5 nm were observed for COMC. From the physicochemical properties summarized in Table 1, it can be seen that the pore size, surface area and

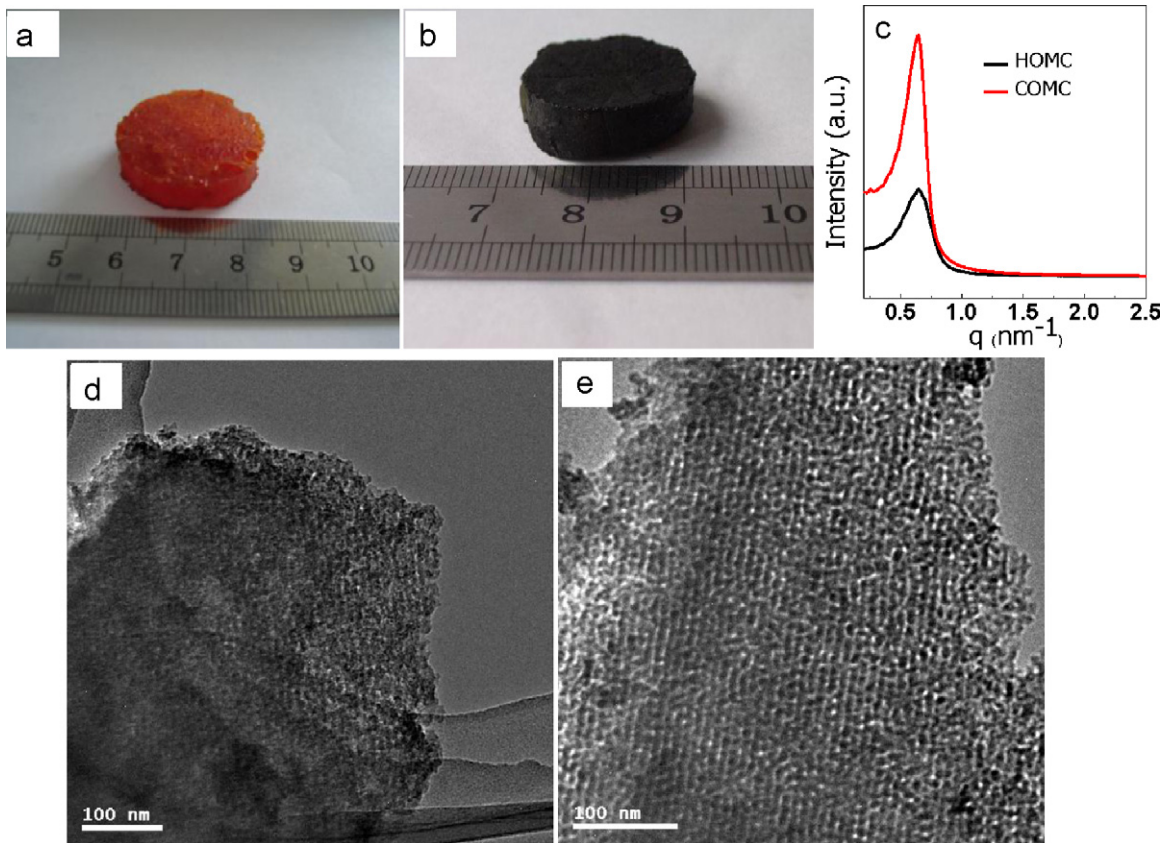


Fig. 1. Photographs of monolithic polymer (a) and carbon (b), and SAXS patterns (c) and TEM images of HOMC (d) and COMC (e).

pore volume enlarged when citric acid used as catalyst instead of HCl. The t -plot calculation reveals that the micropore volume of COMC is a little larger than that of HOMC. Since citric acid can enhance the hydrogen bond interaction between template and resins, the PEO segments of triblock copolymers could be embedded into the resins during polymerization process, and the microporosity in the synthesized carbons may result from the removal of PEO block which makes some disfigurement in the pore wall of the final products [21]. Thus, one can see that mesoporous carbon with ordered hexagonal pore structure and large surface area can be fabricated in the presence of citric acid.

Catalytic dehydrogenation of propane is an important route for propylene synthesis. Herein, the mesoporous carbons HOMC

and COMC were tested as catalysts for DH of propane to propylene. For comparison, three other types of carbon materials, AC, carbon nanotubes (CNTs) and graphitic carbon (GC), were also investigated. The activity of the catalyst samples for DH of propane was tested in a fixed-bed tubular reactor at atmospheric pressure at 673–873 K. In addition to propylene being the target product, methane, ethane and ethylene are also formed as by-products over all the carbon catalysts. The C-balance of the inlet and outlet stream indicates that lower hydrocarbons are cracking products. Among these by-products, methane is the most dominating followed by ethane and ethylene. Fig. 3 shows the initial activity at different temperatures over different carbon catalysts. The conversion of propane increased with the elevated reaction temperature, but the

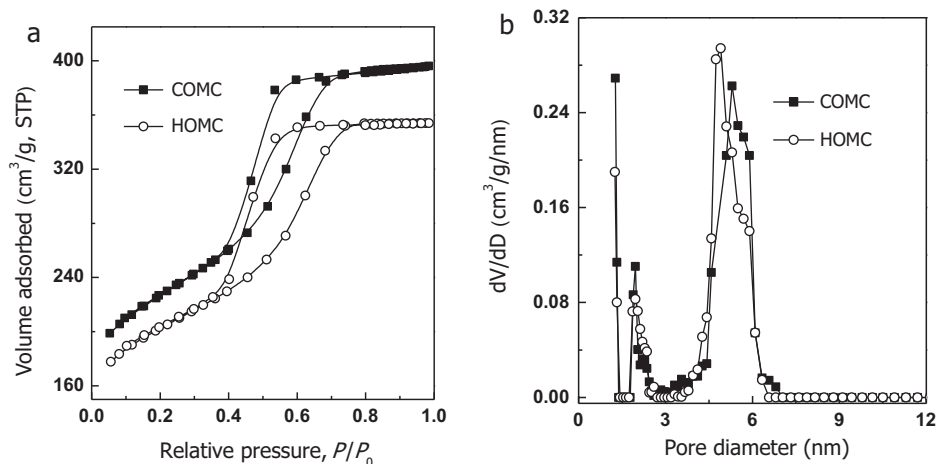


Fig. 2. Nitrogen sorption isotherms (a) and the corresponding pore size distribution curves (b) of HOMC and COMC.

Table 1
Textural properties and specific catalytic activities of different carbon catalysts.^a

Sample	S_{BET} (m ² /g)	$D_{\text{DFT}}^{\text{b}}$ (nm)	$V_{\text{Micro}}^{\text{c}}$ (cm ³ /g)	Reaction rate ^d (mmol/g/h)	Hydrogen yield (mmol/g/h)	Propane conversion (%)		Propylene selectivity (%)	
						Initial	50 h	Initial	50 h
HOMC	675 (325)	4.7	0.14 (0.02)	35.1	32.2	20.1	10.3	66.1	78.5
COMC	758 (405)	5.1	0.16 (0.03)	51.3	47.8	22.6	12.1	89.0	95.1
AC ^e	956 (427)	1–12	0.29 (0.04)	18.3	16.7	17.7	5.2	53.3	74.6
CNTs	212	2–20	0	18.8	17.1	9.0	–	87.5	–
GC ^e	4	–	0	13.4	12.5	6.5	–	93.9	–
COMC ^f	758 (447)	5.1	0.16 (0.01)	14.5	–	21.6	20.1	25.2	25.8

^a Data in the parentheses are for the used catalysts after 50 h of reaction.

^b The pore diameter is calculated using NLDFT method.

^c The micropore volume is calculated from the *t*-plot method.

^d The reaction rates were obtained after reaction for 2 h depicted as propylene formation.

^e AC and GC were purchased from Tianjin Chemical Corp.

^f The data present were obtained when COMC was used as catalyst for ODH.

selectivity to propylene slightly decreased for both HOMC and COMC. The conversions of propane for COMC are 15.9% and 22.6% at 823 and 873 K, respectively. Slightly lower conversions were observed for HOMC, which are 13.9% and 20.1% at 823 and 873 K, respectively. It is worthwhile to note that the selectivity of propylene over HOMC is much lower than that on COMC, which may be due to its poorly ordered mesoporous structure, hindering the transmission of propylene and impeding its releasing from the pore system. Much lower catalytic activities were observed for other carbons with conversions between 5% and 14.0% at 873 K, although the higher selectivity to propylene occurred at higher temperature range.

Fig. 4 shows the results of propane conversion and selectivity to propylene as a function of time over different carbon catalysts. After a short induction period, COMC, HOMC and AC stably catalyze the propylene formation during a reaction lasting 50 h under the operating conditions (Fig. 4a). The final propane conversions are 12.1%, 10.3% and 5.2% for COMC, HOMC and AC, with the final propylene selectivity of 95.2%, 78.5% and 74.6%, respectively. Whereas, severe deactivation of the nanostructured carbons were detected (Fig. 4b). After 10 h, the conversion of propane is as low as 4.5% over CNTs, yielding 4.4% propylene. GC is much less active with propane conversion of 2.4%, yielding 1.4% propylene after only 4 h on stream. The reaction rate as the amount of propylene produced per hour is presented in Table 1, COMC displays a value of 51.3 mmol/g/h, up to approximately 1.5 times of HOMC, and 3–4 times of other tested carbons. COMC is much more active than other carbon materials, displaying a superior catalytic performance. Its catalytic activity is comparable with the binary In–Al–O nanocomposites for the dehydrogenation of propane in the presence of CO₂ or NO₂, afford-

ing steady propane conversion approximately 20% during 30 h on stream [22–24].

Numerous studies on the improvement of existing chromia and platinum based catalysts and the development of vanadia-based and Sn-promoted catalysts have been reported [25–32]. However, the major challenges associated with these catalytic systems are the coking and cracking which influence the catalyst stability and propylene selectivity, respectively. It is worthwhile to note that the propylene selectivity is higher than 90% and remained almost unchanged for COMC over 50 h (Fig. 4a), which is much higher than the K or Na promoted Pt/Sn catalysts with propylene selectivity of only 10–30% [25,26]. The catalytic stability of COMC measured by the reduction of propylene yield is 42.5% after 50 h, which is superior to the extensively discussed Pt-based catalysts supported on amorphous supports or zeolites for propane dehydrogenation, with the reduction of propylene yield of 31.7% after only 4 h time-on-stream [27,28]. Rare earth metals (La, Ce, Y) have been added to Pt–Sn/Al₂O₃ catalysts to enhance the tolerance against catalyst deactivation. However, the dehydrogenation performance of the rare earth metals promoted Pt–Sn catalysts is still not satisfactory, with the propylene yield reduced from 48% to 28.8% over the La promoted catalysts after 2 h [29].

The carbon sample COMC was also tested for ODH of propane to propylene, and the result is shown in Fig. 5. It is remarkable that the conversion and selectivity increased with the temperature. The conversion of propane increased from 10.4% to 21.6%, when the temperature was changed from 623 to 673 K, while the selectivity of propylene slightly increased from 20.1% to 25.2%. As the long term stability test as a function of time-on-stream shown in Fig. 6, after a short induction time at 673 K and at a flow rate of 50 mL/min,

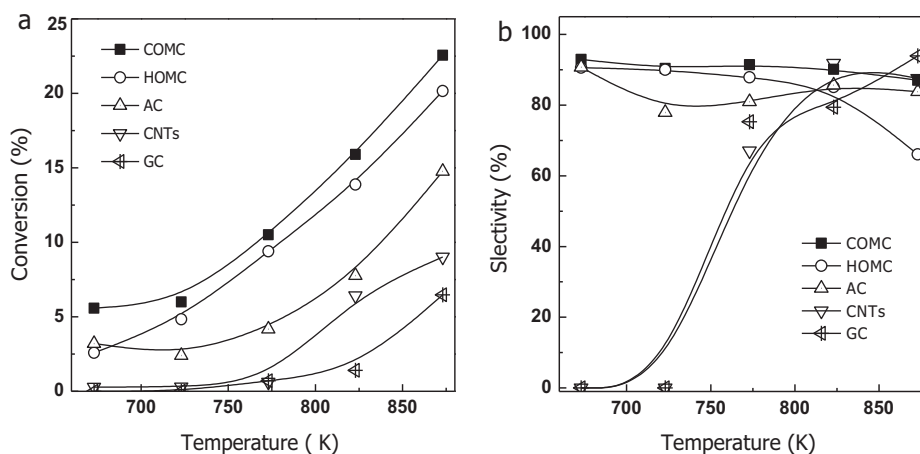


Fig. 3. The initial activity of DH process at different temperatures over different carbon catalysts. (a) Propane conversion and (b) selectivity of propylene.

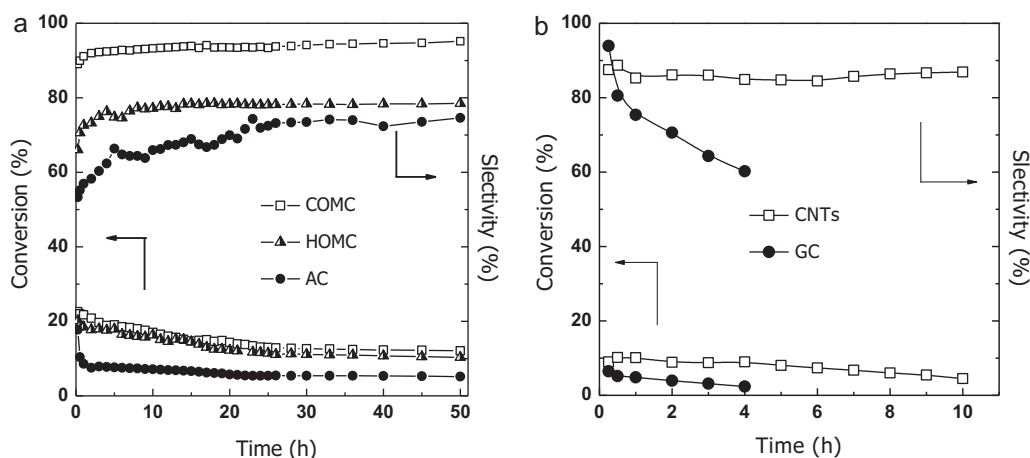


Fig. 4. Propane conversion and propylene selectivity in the DH of propane to propylene over different carbon catalysts. (a) Mesoporous carbons (COMC and HOMC) and AC, and (b) CNTs and GC. Reaction conditions: 0.40 g, 873 K, 5 vol% propane in nitrogen, 40 mL/min.

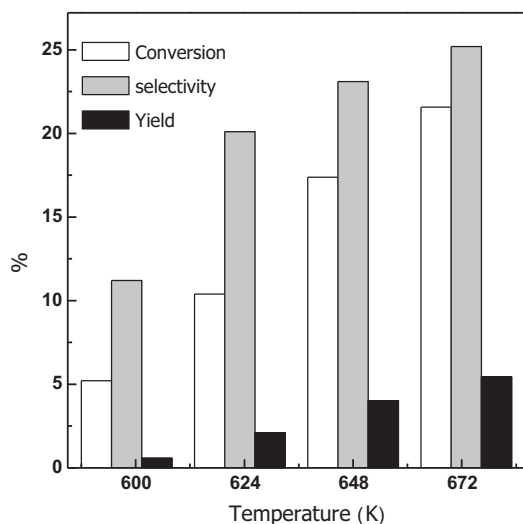


Fig. 5. Conversion, selectivity and yield of ODH of propane to propylene over carbon sample COMC at different temperatures.

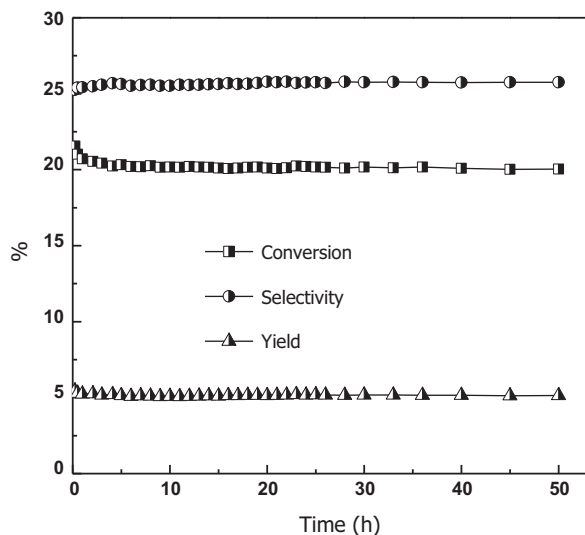


Fig. 6. Conversion, selectivity and yield of ODH of propane to propylene over COMC at 673 K.

a steady propylene selectivity of 25.4% is achieved at a conversion of 21.2%. The high activity at the beginning of the reaction is accompanied by a slightly lower selectivity, but both level-off after 2 h. The highly ordered COMC carbon is structurally stable during the catalytic test of 50 h time-on-steam. AC was also tested for ODH of propane to propylene, however, it yielded only cracked products due to unavoidable combustion in the ODH process with high flow rate [5,33–35].

COMC exhibited a very low selectivity to propylene in the ODH process. It seems that the high surface area of COMC would lead to the re-adsorption of the propylene even for short retention times, rendering a further reaction with oxygen and therefore, a total oxidation in the oxidizing feed-gas atmosphere (50 mL/min flow gas with $C_3H_8:O_2:N_2 = 1:1:8$). This result is consistent with the previously reported CNTs used as catalyst for ODH of propane, while the active sites generated in the oxidizing feed-gas atmosphere are unselective and favor CO_2 formation due to deep oxidation [6].

The robust catalytic activity of COMC and HOMC may be related with their abundant surface oxygen groups. It is generally assumed that each type of surface oxygen groups decomposes to a defined product at different temperatures through temperature-programmed methods. The acidic groups decomposed at low temperatures ($T < 900$ K) and basic groups decomposed

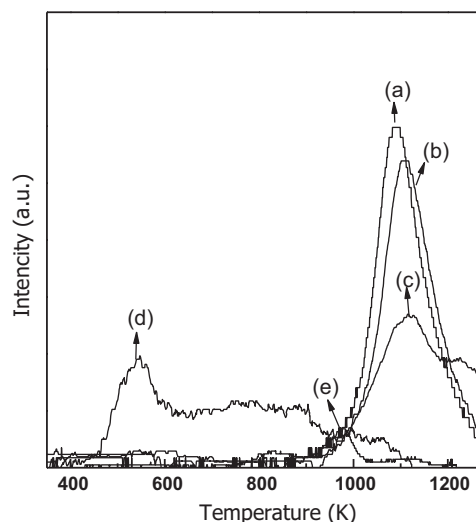


Fig. 7. TPD profiles of different carbons before reaction: (a) COMC, (b) HOMC, (c) AC, (d) CNTs and (e) GC.

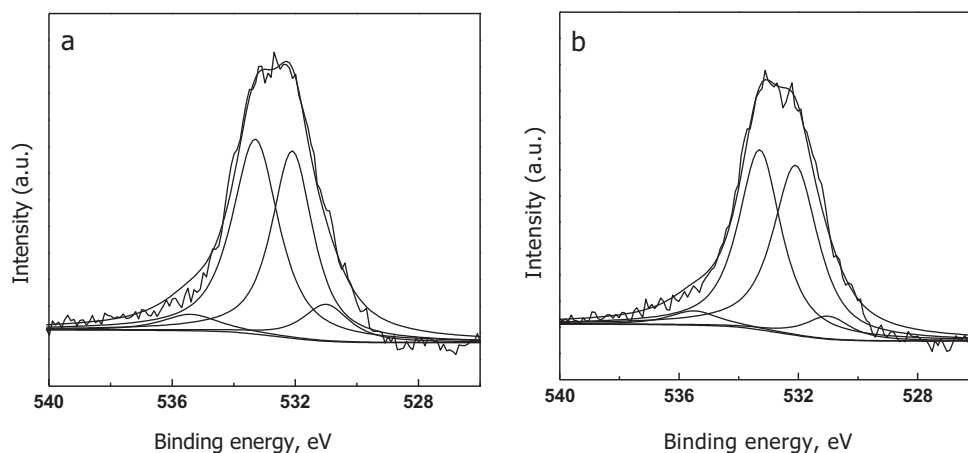


Fig. 8. XPS oxygen 1s spectra of samples COMC (a) and HOMC (b) before reaction. The spectra were normalized in the same intensity.

at temperatures above 900 K [36–39]. The TPD profiles of COMC, HOMC and AC exhibit one peak with maximum at around 1070 K (Fig. 7), which originated from carbonyls and quinone groups, although the intensity of AC is much lower than that of COMC. Nanostructured carbons were also applied to the TPD test. However, CNTs exhibit an extremely small peak at 550 K, corresponding to the carboxylic acid groups, and a very broad peak ranging from 600 to 1100 K, attributing to lactones, anhydrides, phenol and carbonyl groups arising from HNO_3 treatment during the synthesis process [36]. GC represents no obvious peak in the tested temperature, indicating that there are little functional groups in the carbon surfaces, which may cause poor catalytic activity in the dehydrogenation of propane.

The O 1s X-ray photoelectron spectra (XPS) of COMC and HOMC confirm their oxygen-containing surface (Fig. 8). The deconvolution of the O 1s spectrum reveals three different chemical environments of oxygen, which could be assigned to unsaturated C=O components (531.0 eV), C–OH and C=O in anhydrides (532.1 eV), C–O in esters and anhydrides (533.3 eV) and adsorbed water (535.4 eV) [40]. The total surface oxygen atomic concentrations in the samples COMC and HOMC were estimated from XPS spectra to be 4.5% and 4.0%, respectively, and the corresponding unsaturated C=O concentrations are 0.4%, and 0.25%, respectively. The presence of basic sites has been reported as active sites during the dehydrogenation reaction [6,41,42]. The sample with the highest carbonyl concentration has the highest reaction rate, corresponding to the fact that carbonyl–quinone groups are the active sites in the dehydrogenation reaction [5].

The BET surface area and pore volume of COMC seriously decreased (Table 1, data in the parentheses) after both DH and ODH reaction, e.g., the BET surface area of COMC decreased from 758 to 405 m^2/g after used as catalyst for DH process. Meanwhile, it is worthwhile to note that the micropores nearly disappeared for COMC carbon catalysts after long time reaction, which may be the result of the formation of coke during the reaction [35]. The values of carbon balance in the calculation between propane conversion and the formed products slightly higher than unit also indicated the coke formation during the reactions. Correspondingly, a slight deactivation process was observed. However, the high stability shown in Table 1 indicates that the loss of the surface area at the very beginning of the reaction did not have a strong influence to the catalytic performance of the carbon catalysts. The coke formation at the beginning of the reaction may be an active phase as reported by Cadús et al. for Al_2O_3 [43].

COMC used for both DH and ODH of propane exhibits an unusual stability that can be related with its unique structure: the larger, but well-ordered porosity of mesoporous carbon is advantageous

for mass transport and good thermal stability [35]. AC is also active in the DH of propane to propylene, but deactivates sharply at the very beginning, although both carbon materials are characteristic for the high-surface area. This may be as a result of the formed coke blocking most of the micropores of AC and overlapping the active sites. The specific surface area of the used COMC carbon after the DH reaction is still as high as 405 m^2/g , while the specific surface area of activated carbon typically decreased from 956 to 427 m^2/g .

The metal-oxides bring pollution to environment and the noble metal based catalysts are expensive. The ordered mesoporous carbons present high catalytic activity and stability in the dehydrogenation of propane, which is promising as an alternative to metal-oxide catalysts and noble metal based catalysts for dehydrogenation reactions of alkanes.

4. Conclusions

A simple and environmentally benign method to prepare monolithic OMCs was proposed from self-assembly of resorcinol–formaldehyde and block copolymers catalyzed by citric acid. Well-ordered hexagonal structure was obtained as a result of the enhanced driving force provided by citric acid, while poorly ordered mesostructure was obtained when HCl was used at the same conditions. The prepared ordered mesoporous carbons exhibited high activity in dehydrogenation of propane to propylene. The basic oxygen groups are the active sites for selective dehydrogenation. The regeneration of the active sites is achieved by oxidation of C–OH in ODH process and thermal dehydrogenation in DH process.

Acknowledgements

This work was supported by the National Natural Science Foundation of China (20973096, 21076056), the National Basic Research Program of China (2009CB623502), and the Program for Changjiang Scholars and Innovative Research Team in University (IRT0927).

Appendix A. Supplementary data

Supplementary data associated with this article can be found, in the online version, at doi:10.1016/j.cattod.2011.08.022.

References

- [1] M.F.R. Pereira, J.J.M. Orfao, J.L. Figueiredo, Appl. Catal. A: Gen. 184 (1999) 153–160.
- [2] M.F.R. Pereira, J.J.M. Orfao, J.L. Figueiredo, Appl. Catal. A: Gen. 196 (2000) 43–54.
- [3] J.J. Delgado, D.S. Su, G. Reibmann, N. Keller, A. Gajovic, R. Schlögl, J. Catal. 244 (2006) 126–129.

- [4] J. Zhang, X. Liu, R. Blume, A.H. Zhang, R. Schlögl, D.S. Su, *Science* 322 (2008) 73–78.
- [5] J. Zhang, D.S. Su, A.H. Zhang, D. Wang, R. Schlögl, C. Hébert, *Angew. Chem. Int. Ed.* 46 (2007) 7319–7323.
- [6] B. Frank, J. Zhang, R. Blume, R. Schlögl, D.S. Su, *Angew. Chem. Int. Ed.* 48 (2009) 6913–6917.
- [7] G. Mestl, N.I. Maksimova, N. Keller, V.V. Roddatis, R. Schlögl, *Angew. Chem. Int. Ed.* 40 (2001) 2066–2068.
- [8] D.S. Su, N.I. Maksimova, G. Mestl, V.L. Kuznetsov, V. Keller, R. Schlögl, N. Keller, *Carbon* 45 (2007) 2145–2151.
- [9] C.D. Liang, H. Xie, V. Schwartz, J. Howe, S. Dai, S.H. Overbury, *J. Am. Chem. Soc.* 131 (2009) 7735–7741.
- [10] B. Frank, M. Morassutto, R. Schomcker, R. Schlögl, D.S. Su, *ChemCatChem* 2 (2010) 644–648.
- [11] S. Jun, S.H. Joo, R. Ryoo, M. Kruk, M. Jaroniec, Z. Liu, T. Ohsuna, O. Terasaki, *J. Am. Chem. Soc.* 122 (2000) 10712–10713.
- [12] R. Ryoo, S.H. Joo, M. Kruk, M. Jaroniec, *Adv. Mater.* 13 (2001) 677–681.
- [13] R. Ryoo, S.H. Joo, S. Jun, *J. Phys. Chem. B* 103 (1999) 7743–7746.
- [14] C.D. Liang, K.L. Hong, G.A. Guiochon, J.W. Mays, S. Dai, *Angew. Chem. Int. Ed.* 43 (2004) 5785–5789.
- [15] S. Tanaka, N. Nishiyama, Y. Egshira, K. Ueyama, *Chem. Commun.* (2005) 2125–2127.
- [16] Y. Meng, D. Gu, F. Zhang, Y. Shi, H. Yang, Z. Li, C. Yu, B. Tu, D. Zhao, *Angew. Chem. Int. Ed.* 44 (2005) 7053–7058.
- [17] F. Zhang, Y. Meng, D. Gu, Y. Yan, C. Yu, B. Tu, D. Zhao, *J. Am. Chem. Soc.* 127 (2005) 13508–13509.
- [18] Y. Huang, H. Cai, T. Yu, F. Zhang, F. Zhang, Y. Meng, D. Gu, Y. Wan, X. Sun, B. Tu, D. Zhao, *Angew. Chem. Int. Ed.* 46 (2007) 1089–1093.
- [19] L. Liu, F.Y. Wang, G.S. Shao, Z.Y. Yuan, *Carbon* 48 (2010) 2089–2099.
- [20] A.H. Lu, B. Spliethoff, F. Schüth, *Chem. Mater.* 20 (2008) 5314–5319.
- [21] D.Y. Zhao, Q.S. Huo, J.L. Feng, B.F. Chmelka, G.D. Stucky, *J. Am. Chem. Soc.* 120 (1998) 6024–6036.
- [22] M. Chen, J. Xu, Y. Cao, H.Y. He, K.N. Fan, J.H. Zhuang, *J. Catal.* 272 (2010) 101–108.
- [23] M. Chen, J. Xu, Y.M. Liu, Y. Cao, H.Y. He, J.H. Zhuang, *Appl. Catal. A: Gen.* 377 (2010) 35–41.
- [24] M. Chen, J.L. Wu, Y.M. Liu, Y. Cao, K.N. Fan, *Catal. Commun.* 12 (2011) 1063–1066.
- [25] S.B. Zhang, Y.M. Zhou, Y.W. Zhang, L. Huang, *Catal. Lett.* 135 (2010) 76–82.
- [26] Z.Y. Duan, Y.M. Zhou, Y.W. Zhang, X.L. Sheng, M.W. Xue, *Catal. Lett.* 141 (2011) 120–127.
- [27] L.H. Huang, B.L. Xu, L.L. Yang, Y.N. Fan, *Catal. Commun.* 9 (2008) 2593–2597.
- [28] M.S. Kumar, D. Chen, A. Holmen, J.C. Walmsley, *Catal. Today* 142 (2009) 17–23.
- [29] B.K. Vu, M.B. Song, I.Y. Ahn, Y.W. Suh, D.J. Suh, W. Kim, H.L. Koh, Y.G. Choi, E.W. Shin, *Catal. Today* 164 (2011) 214–220.
- [30] J.M. McNamara, S.D. Jackson, D. Lennon, *Catal. Today* 81 (2003) 583–587.
- [31] J.N.J. van Lingen, O.L.J. Gijzeman, B.M. Weckhuysen, J.H. van Lenthe, *J. Catal.* 239 (2006) 34–41.
- [32] M.L. Ferreira, M. Volpe, *J. Mol. Catal. A Chem.* 164 (2000) 281–290.
- [33] M.S. Kane, L.C. Kao, R.K. Mariwala, D.F. Hilscher, H.C. Foley, *Ind. Eng. Chem. Res.* 35 (1996) 3319–3331.
- [34] M.F.R. Pereira, J.J.M. Órfão, J.L. Figueiredo, *Appl. Catal. A* 218 (2001) 307–318.
- [35] D.S. Su, J.J. Delgado, X. Liu, D. Wang, R. Schlögl, L.F. Wang, Z. Zhang, Z.C. Shan, F.S. Xiao, *Chem. Asian J.* 4 (2009) 1108–1113.
- [36] U. Zielke, K.J. Hutter, W.P. Hoffman, *Carbon* 34 (1996) 983–998.
- [37] B. Marchon, J. Carrazza, H. Heinemann, G.A. Somorjai, *Carbon* 26 (1988) 507–514.
- [38] Y. Xie, P.M.A. Sherwood, *Chem. Mater.* 2 (1990) 293–299.
- [39] H.F. Gorgulho, J.P. Mesquita, F. Gonçalves, M.F.R. Pereira, J.L. Figueiredo, *Carbon* 46 (2008) 1544–1555.
- [40] J.L. Figueiredo, M.F.R. Pereira, *Catal. Today* 150 (2010) 2–7.
- [41] J. Zhang, D.S. Su, R. Blume, R. Schlögl, R. Wang, X. Yang, *Angew. Chem. Int. Ed.* 49 (2010) 8640–8644.
- [42] X. Liu, B. Frank, W. Zhang, T.P. Cotter, R. Schlögl, D.S. Su, *Angew. Chem. Int. Ed.* 50 (2011) 3318–3322.
- [43] L.E. Cadús, L.A. Arrua, O.F. Gorrioz, J.B. Rivarola, *Ind. Eng. Chem. Res.* 27 (1988) 2241–2246.